Irisin, a Novel Myokine, Regulates Glucose Uptake in Skeletal Muscle Cells via AMPK

Hye Jeong Lee, Jung Ok Lee, Nami Kim, Joong Kwan Kim, Hyung Ip Kim, Yong Woo Lee, Su Jin Kim, Jong-Il Choi, Yoonji Oh, Jeong Hyun Kim, Suyeon-Hwang, Sun Hwa Park, and Hyeon Soo Kim

Department of Anatomy (H.J.L., J.O.L., N.K., J.K.K., H.I.K., Y.W.L., S.J.K., S.H.P., H.S.K.), Korea University College of Medicine, Seoul, Korea 136-705; Division of Cardiology (J.-I.C.), Department of Internal Medicine, Korea University Medical Center, Seoul, Korea; College of Nursing (Y.O.), Korea University, Seoul, Korea 136-705; College of Pre-Pharm·Med (J.H.K.), DukSung Women's University, Seoul, Korea 132-714; and College of Pharmacy (S.-H.), University of Rhode Island, Kingston, Rhode Island 02881

Irisin is a novel myokine produced by skeletal muscle. However, its metabolic role is poorly understood. In the present study, irisin induced glucose uptake in differentiated skeletal muscle cells. It increased AMP-activated protein kinase (AMPK) phosphorylation and the inhibition of AMPK blocked glucose uptake. It also increased reactive oxygen species (ROS) generation. N-acetyl cysteine, a ROS scavenger, blocked irisin-induced AMPK phosphorylation. Moreover, irisin activated p38 MAPK in an AMPK-dependent manner. The inhibition and knockdown of p38 MAPK blocked irisin-induced glucose uptake. A colorimetric absorbance assay showed that irisin stimulated the translocation of glucose transporter type 4 to the plasma membrane and that this effect was suppressed in cells pretreated with a p38 MAPK inhibitor or p38 MAPK small interfering RNA. In primary cultured myoblast cells, irisin increased the concentration of intracellular calcium. STO-609, a calcium/calmodulin-dependent protein kinase kinase inhibitor, blocked irisin-induced AMPK phosphorylation, implying that calcium is involved in irisin-mediated signaling. Our results suggest that irisin plays an important role in glucose metabolism via the ROS-mediated AMPK pathway in skeletal muscle cells. **(*Molecular Endocrinology* 29: 873–881, 2015)**

AMP-activated protein kinase (AMPK) is an evolutionary conserved and ubiquitously expressed kinase that plays an important role in cellular energy homeostasis. It is a heterotrimeric complex consisting of a catalytic subunit (α) and 2 regulatory subunits (β and γ) and is activated upon depletion of cellular energy stores (1) through the phosphorylation of Thr^{172} on the catalytic subunit by AMPK kinase. When the AMP to ATP ratio rises, AMP binds to the γ-subunit and causes a conformational change in the heterotrimer, making the α-subunit a substrate for upstream kinases. Liver kinase B1 and calcium/calmodulin-dependent protein kinase kinase (CaMKK)β have been identified as upstream kinases (2–5). In addition, AMPK activation through physiological stimulation such as muscle contraction or the pharmacological activator, 5-aminoimidazole-4-carboxamide-1-day-ribofuranoside, results in a significant increase in glucose uptake, which is mediated by the translocation of glucose transporter type 4 (GLUT4) (6, 7). GLUT4 is highly expressed in adipose tissue and skeletal muscle (8, 9) and mediates the removal of circulating glucose. Therefore, it is a key regulator of systemic glucose homeostasis (10). One recent study demonstrated that mice with myostatin knockout exhibited increased muscle mass and reduced fat mass through AMPK activation (11), suggesting that myostatin represents a therapeutic target for obesity and diabetes. Although myokines have been the focus of research in terms of their relationship with AMPK as mo-

ISSN Print 0888-8809 ISSN Online 1944-9917
Printed in USA

Received November 5, 2014. Accepted March 26, 2015.
First Published Online March 31, 2015

Abbreviations: ACC, acetyl-CoA carboxylase; AMPK, AMP-activated protein kinase; CaMKK, calcium/calmodulin-dependent protein kinase kinase; DCF-DA, 2′7′-dichlorodihydrofluorescein diacetate; FNDC5, fibronectin type III domain-containing 5; GLUT4, glucose transporter type 4; HRP, horseradish peroxidase; NAC, N-acetyl cysteine; PGC, peroxisome proliterator-activator receptor γ coactivator; ROS, reactive oxygen species; siRNA, small interfering RNA.

lecular targets for cellular energy sensors, many details on their molecular mechanism remain unclear. Therefore, further study is necessary to understand the function of myokines in the process of signal transduction.

Skeletal muscle is the largest organ of the body and is characterized by its mechanical roles in posture and movement. However, recent evidence demonstrated that skeletal muscle is not only an organ for locomotion but also plays a role in the secretion of physiological factors. Many types of peptide are produced, expressed, and secreted by skeletal muscles, and they are classified as myokines (12). The myokine secretome consists of various types of cytokines that communicate with other organs, such as adipose tissue, the liver, and the brain, in an autocrine, paracrine, or endocrine manner (13). So far, various types of myokines have been identified, such as IL-6 (14), fibroblast growth factor-21 (15), insulin-like 6, follistatin-like 1 (16), Leukemia inhibitory factor (17), IL-7 (18), IL-15 (19), musclin (20), and irisin (21). Myokines are known to be involved in various physiological functions, such as myogenesis (22), fat oxidation (23), osteogenesis (24), endothelial function (25), and fat browning (21). They are secreted in response to muscle contraction. Therefore, they could provide a useful clue to understanding the relationship between myokines and chronic diseases related to physical inactivity, such as obesity and diabetes.

A recent study demonstrated that physical exercise induced peroxisome proliferator-activator receptor γ coactivator (PGC) 1α and its downstream membrane protein, fibronectin type III domain-containing 5 (FNDC5), which is cleaved to form irisin (21). Many physiological functions of irisin have previously been reported, such as white fat browning (26), thermogenesis (27), and uncoupling protein 1 induction (28). Thus, it is tempting to speculate that irisin has the capacity to regulate glucose homeostasis in skeletal muscle systems in an autocrine manner.

In this study, the effects of irisin on AMPK were examined to determine its role in hypoglycemia. Irisin was found to stimulate glucose uptake in skeletal muscle cells by a mechanism involving the reactive oxygen species (ROS)-mediated AMPK pathway. These results provide novel insights into the contribution of irisin to glucose metabolism in skeletal muscle cells.

Materials and Methods

Reagents

Antibodies against AMPK, phospho-AMPK (Thr^{172}), acetyl-CoA carboxylase (ACC), and phosphor-ACC (Ser^{79}) were from Millipore-Upstate; p38 MAPK and phospho-p38 MAPK (Thr^{180}/Tyr^{182}) from Santa Cruz; and myogenin was purchased from Epitomics, Inc. Horseradish peroxidase (HRP)-conjugated secondary antibodies were from Enzo Life Sciences. Compound C, 5-aminoimidazole-4-carboxamide-1-day-ribofuranoside, SB202190, insulin, and N-acetyl cysteine (NAC) were obtained from Calbiochem. Irisin was purchased from Phoenix Pharmaceuticals. The fluorescent ROS indicator 2′7′-dichlorodihydrofluorescein diacetate (DCF-DA) was obtained from Invitrogen.

Cell culture

L6 muscle cells were maintained in DMEM (Invitrogen) supplemented with 10% fetal bovine serum and antibiotics (37°C; 5% CO_2).

Immunoblot analysis

L6 cells were grown in 6-well plates and subjected to serum-starvation for 5 hours before treatment. After the experimental manipulations, the medium was removed, and the cells were washed twice with ice-cold PBS and lysed with 60 μL of lysis buffer. The samples were sonicated, heated for 5 minutes at 95°C, and then centrifuged for 25 minutes. The supernatants were resolved on sodium dodecyl sulfate-PAGE (8%) gels then transferred to polyvinylidene difluoride membranes, which were incubated overnight at 4°C with primary antibodies. After 6 washes in Tris-buffered saline containing 0.1% Tween 20, the membranes were incubated for 1 hour with HRP-conjugated secondary antibodies at room temperature. The blots were washed and then visualized by chemiluminescence using the Amersham Biosciences enhanced chemiluminescence Western blotting detection system (Amersham International PLC). The membrane was scanned and densitometry analysis was performed with an ImageJ analysis.

Knockdown of p38 MAPK and AMPKα2 by using small interfering RNA (siRNA)

L6 cells were seeded on 6-well plates and grown to 70% confluence over 24 hours. Transient transfections were performed using Lipofectamine 2000 (Invitrogen) according to the manufacturer's protocol. Briefly, siRNA for p38 MAPK (L-080059-02-0005; Thermo Scientific), AMPKα2 (NM_001013367; Dharmacon), and a nontargeted control siRNA were purchased from Bioneer. The 5 μL of siRNA and 5 μL of Lipofectamine 2000 were each diluted with 95 μL of reduced serum medium (Opti-MEM; Invitrogen), and then combined. The mixtures were incubated for 20 minutes at room temperature before being added dropwise to the culture well containing 800 μL of Opti-MEM. After 4 hours, the medium was replaced with fresh DMEM, and the cells were cultivated for 48 hours.

Immunodetection of GLUT4myc

Cell surface expression of GLUT4myc was quantified using an antibody-coupled colorimetric absorbance assay as previously described (23). After stimulation by insulin or metformin, myoblasts that stably expressed L6-GLUT4myc were incubated with polyclonal anti-myc antibody (1:1000) for 60 minutes. They were then fixed with 4% paraformaldehyde in krebs-ringer bicarbonate for 10 minutes and incubated with HRP-conjugated goat antirabbit IgG (1:1000) for 1 hour. Cells were washed 2 times in PBS, and incubated in 1 mL of O-phemylenediamine dihydrochloride reagent (0.4 mg/mL) for 30 minutes. The absorbance of the supernatant was measured at 492 nm.

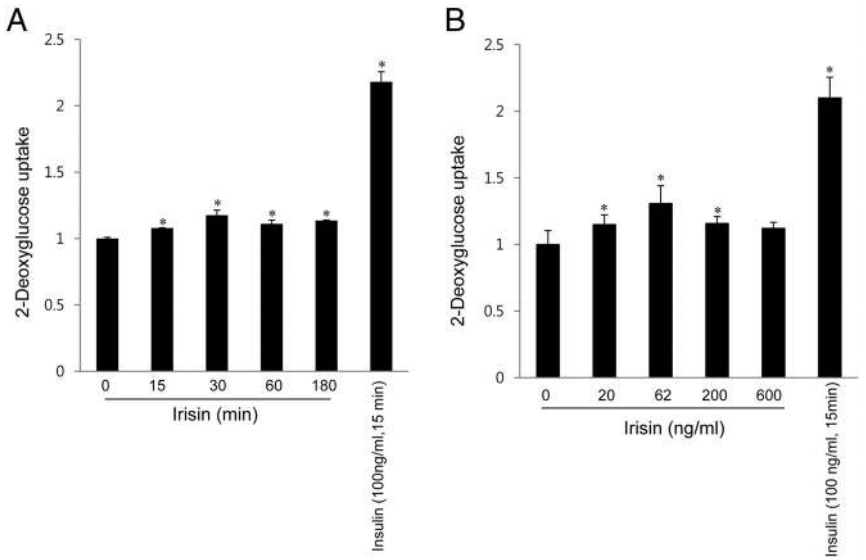

Figure 1. Irisin stimulates glucose uptake in differentiated muscle cells. A, L6 myotube cells were incubated with irisin (62 ng/mL) for the indicated times and then assayed for glucose uptake. B, Differentiated L6 myotube cells were incubated with different concentrations of irisin for 1 hour and then assayed for glucose uptake. Insulin (100 ng/mL) was treated for 15 minutes and used as a positive control. *, $P < .05$ vs basal condition.

Analysis of 2-deoxyglucose uptake

The uptake of 2-deoxyglucose was examined in differentiated L6 muscle cells. Two days after cells reached confluence, differentiation into myotubes was induced by incubation for 6–7 days in DMEM supplemented with 2% fetal bovine serum, which was changed every 2 days. Cells were washed twice in PBS containing 2.5mM $MgCl_2$, 1mM $CaCl_2$, and 20mM HEPES (pH 7.4), then incubated with the test compounds in the same buffer at 37°C. The uptake assay was initiated by adding 0.5 μCi of 2-deoxy-D [H^3] glucose to each well and incubating for 10 minutes at 37°C. The process was terminated by washing the cells with ice-cold PBS. Cells were lysed in 10% sodium dodecyl sulfate for determination of radioactivity.

ROS measurement by using DCF-DA

ROS concentration was determined by detecting fluorescence in cells treated with the ROS-sensitive indicator, DCF-DA by using confocal microscopy (Zeiss LSM 510 Meta; Zeiss). L6 cells were loaded with 5mM DCF-DA in regular culture medium for 45 minutes at room temperature. The culture plates were placed on a temperature-controlled microscope stage and examined using the ×20 objective. The excitation and emission wavelengths for signal detection were 488 and 515 nm, respectively.

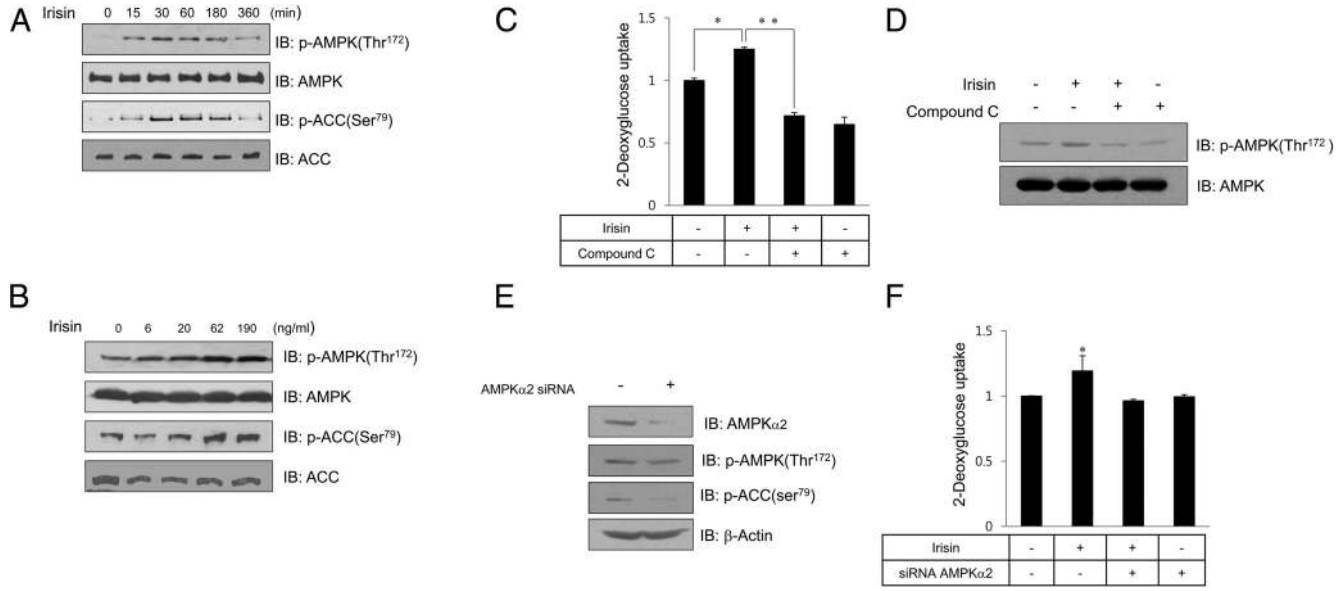

Figure 2. Irisin activates AMPK in L6 cells. A, L6 cells were incubated with irisin (62 ng/mL) for the indicated times. Cell lysates were analyzed by Western blotting, using antibodies against phospho-AMPK (Thr^{172}) and ACC (Ser^{79}), whereas AMPK and ACC served as controls. B, L6 cells were stimulated for 1 hour at several concentrations of irisin. The cell lysates were analyzed by Western blotting using antibody against phospho-AMPK (Thr^{172}) and ACC (Ser^{79}), whereas AMPK and ACC served as controls. C, Differentiated L6 myotube cells were incubated for 1 hour with irisin (62 ng/mL) in the presence of the AMPK inhibitor compound C (2μM) and then assayed for glucose uptake. *, $P < .05$ vs basal condition; **, $P < .05$ vs irisin-treated condition. D, L6 cells were pretreated with compound C (2μM), then incubated with irisin (62 ng/mL) for 60 minutes. Cell lysates were analyzed by Western blotting using an antibody against phospho-AMPK (Thr^{172}), whereas AMPK served as a control. E, L6 cells were transiently transfected with AMPKα2 siRNA for 48 hours. The cell lysates were analyzed by Western blotting using antibody against phosphorylated AMPK2 and ACC, whereas AMPKα2 and β-actin served as controls. F, L6 cells were transiently transfected with AMPKα2 siRNA for 48 hours. Differentiated L6 myotube cells were incubated for 1 hour with irisin (62 ng/mL) and then assayed for glucose uptake. *, $P < .05$ vs basal condition.

Intracellular calcium measurement

Ca^{2+} concentration was determined by detecting fluorescence in cells treated with the Ca^{2+}-sensitive indicator, fluo-3 AM, using confocal microscopy (Zeiss LSM 510 Meta; Zeiss). The cells were loaded with 5mM Fluo-3 AM in regular culture medium for 45 minutes at room temperature. The culture plates were placed on a temperature-controlled microscope stage and observed using the 20× objective lens. The excitation and emission wavelength for signal detection was 488 nm.

Primary myoblast preparation

We isolated primary myoblasts from the forelimbs and hindlimbs of 3–4 5-day-old littermate pups. The dissected and minced muscle was enzymatically disaggregated in 4 mL PBS containing 1.5-U/mL dispase II and 1.4-U/mL collagenase D (Roche), and triturated with a 10-mL pipette every 5 minutes for 20 minutes at 37°C. The cells were filtered through 70-μm mesh (BD) and collected by pelleting at 1000 rpm for 5 minutes. The cell pellet was dissociated in 10 mL of F10 medium (Invitrogen) supplemented with 10 ng/mL of basic fibroblast growth factor (PeproTech) and 10% cosmic calf serum (Hyclone; referred to as growth medium 1. Finally, the cells were preplated onto non-collagen-coated plates twice for 1 hour to deplete the population of fibroblasts, which generally adhere faster than myoblasts. To induce differentiation, primary myoblasts at 75% confluence were placed into DMEM containing antibiotics and 5% horse serum (Invitrogen).

Data analysis

One-way ANOVA and Holm-Sidak comparisons were used to compare each experimental condition. The means were considered statistically different when the probability of the event was determined to be below 5% ($P < .05$).

Results

Irisin stimulates glucose uptake in differentiated muscle cells

Among established skeletal muscle cells, rat myoblast L6 cells could be the most promising model to investigate glucose uptake. The effect of irisin treatment on glucose uptake in differentiated L6 cells was determined. We found that the presence of irisin resulted in increased glucose uptake in these cells. The maximum glucose uptake was observed after 30 minutes of treatment with irisin (Figure 1A). The increase of glucose uptake was maximized at a concentration of 62 ng/mL (Figure 1B). Insulin was used as a positive control. These results indicate that irisin exerts a glucose regulatory role in skeletal muscles.

Irisin activates AMPK in L6 cells

To assess whether AMPK, a key player in glucose uptake, is involved in irisin-mediated signaling, the degree of AMPK phosphorylation in irisin-treated L6 cells was determined. The levels of phospho-AMPK (Thr^{172}) and its downstream ACC were highest at 30 minutes in irisin-treated cells (Figure 2A). In addition, irisin induced a dose-dependent increase in AMPK phosphorylation (Figure 2B). The degree of phosphorylation was maximal at 62 ng/mL of irisin. The presence of the AMPK inhibitor compound C abrogated the observed irisin-induced glucose uptake (Figure 2C). Compound C blocked the irisin-mediated phosphorylation of AMPK, confirm the activity of compound C (Figure 2D). To further confirm, we first knocked down AMPKα2 with siRNA (Figure 2E). Knockdown of AMPKα2 blocked irisin-induced glucose uptake (Figure 2F). These results demonstrate that irisin stimulates glucose uptake via the AMPK pathway.

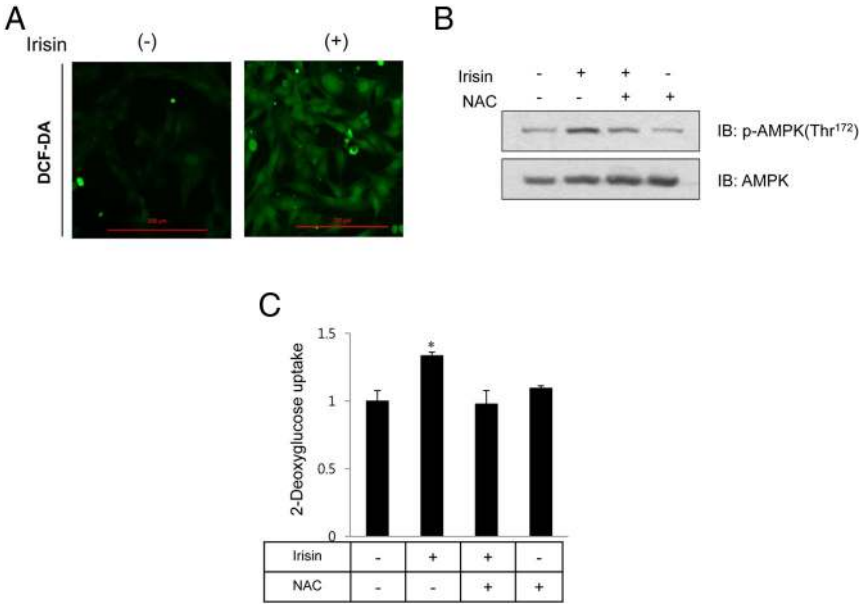

Figure 3. Irisin activates the AMPK signaling pathway through ROS in myoblasts. A, Increase of ROS after irisin treatment. L6 cells were treated with irisin (62 ng/mL) for 1 hour. ROS were stained with the marker DCF-DA. Images were captured using a confocal microscope. B, L6 cells were pretreated with the ROS scavenger NAC for 15 minutes and then incubated with irisin (62 ng/mL) for 1 hour. The cell lysates were analyzed by Western blotting with antibodies against phospho-AMPK (Thr^{172}) and AMPK. C, Differentiated L6 myotube cells were pretreated with the ROS scavenger NAC for 15 minutes, then incubated with irisin (62 ng/mL) for 1 hour, and then assayed for glucose uptake. *, $P < .05$ vs basal condition.

Irisin activates the AMPK signaling pathway through ROS

Some papers demonstrated that ROS was associated with AMPK activation (29, 30). Together with the our finding that irisin increased

ROS, these facts led us to hypothesize that ROS may involve in irisin-mediated AMPK phosphorylation. To elucidate the mechanism of irisin-mediated AMPK phosphorylation, the effects of irisin on the level of the ROS were examined. For the ROS assay, cells were first incubated for 1 hour with irisin, and stained with DCF-DA, a ROS-sensitive dye. Using a confocal microscope, the level of ROS was determined by the fluorescence intensity. The intensity increased after irisin stimulation (Figure 3A), indicating that irisin increased the ROS level in L6 cells. To clarify the role of ROS in AMPK phosphorylation, ROS were chelated using the ROS scavenger, NAC. This resulted in a decrease in AMPK phosphorylation (Figure 3B). NAC blocked the irisin-mediated glucose uptake (Figure 3C). These results demonstrate that irisin increases AMPK phosphorylation through ROS generation.

The p38 MAPK pathway is involved in irisin-mediated glucose uptake

Previous articles showed that AMPK played as p38 MAPK upstream (31, 32) and p38 MAPK played as an upstream for GLUT4 translocation (33, 34). Thus, we speculated that irisin might stimulate glucose uptake via p38 MAPK pathway. To prove this hypothesis, the effect

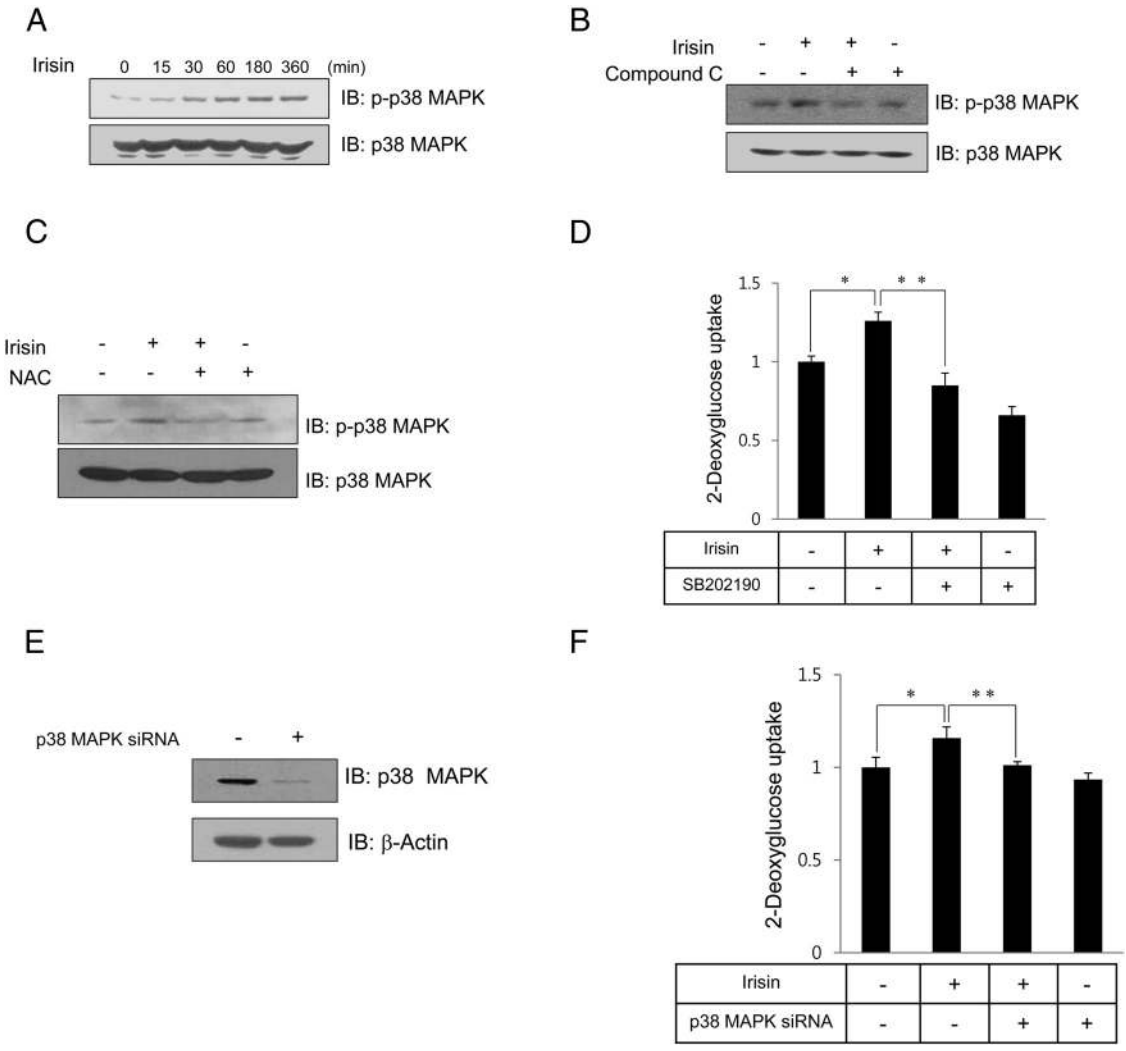

Figure 4. The p38 MAPK pathway is involved in irisin-mediated glucose uptake. A, L6 cells were incubated with irisin (62 ng/mL) for the indicated times. Lysates were analyzed by Western blotting using an antibody against phospho-p38 MAPK, whereas p38 MAPK served as a control. B, L6 cells were pretreated with compound C (2μM), then incubated with irisin (62 ng/mL) for 60 minutes. Cell lysates were analyzed by Western blotting using an antibody against phospho-p38 MAPK, whereas p38 MAPK served as a control. C, L6 cells were pretreated with the ROS scavenger NAC for 15 minutes and then incubated with irisin (62 ng/mL) for 1 hour. The cell lysates were analyzed by Western blotting with antibodies against phospho-p38 MAPK and p38 MAPK. D, Differentiated L6 myotube cells were incubated with irisin (62 ng/mL) for 1 hour in the presence of the p38 MAPK inhibitor SB202190 (5μM), before assaying for glucose uptake. E, L6 cells were transiently transfected with p38 MAPK siRNA for 48 hours. The cell lysates were analyzed by Western blotting using antibody against p38 MAPK, whereas β-actin served as controls. F, Differentiated L6 myotube cells were transiently transfected with p38 MAPK siRNA (50nM) for 48 hours and then incubated with irisin (62 ng/mL) for 1 hour before assaying for glucose uptake. *, $P < .05$ vs basal condition; **, $P < .05$ vs irisin-treated condition.

of irisin on the phosphorylation of p38 MAPK was examined. Irisin treatment resulted in a time-dependent increase in p38 MAPK phosphorylation in L6 cells (Figure 4A). The presence of the AMPK inhibitor abrogated the observed irisin-induced increase of p38 MAPK phosphorylation (Figure 4B). NAC blocked the irisin-mediated p38 MAPK phosphorylation (Figure 4C). In addition, the irisin-induced uptake of glucose was abolished upon treatment with SB202190, a p38 MAPK inhibitor (Figure 4D). To confirm that the effects of irisin were due to p38 MAPK phosphorylation, p38 MAPK was knocked down using siRNA (Figure 4E). Irisin-mediated glucose uptake was decreased in p38 MAPK siRNA-transfected cells (Figure 4F), indicating that irisin mediates glucose uptake through p38 MAPK. Inhibition of p38 MAPK did not change irisin-mediated AMPK phosphorylation (data not shown), indicated that AMPK play as an upstream molecule of p38 MAPK. These results demonstrate that irisin stimulates glucose uptake via the p38 MAPK pathway.

Irisin stimulates GLUT4 translocation

Based on the finding that irisin can mediate glucose uptake by p38 MAPK activation, the effect of irisin on the expression of GLUT4, a p38 MAPK target, was evaluated. Irisin treatment had no effect on the level of GLUT4 mRNA (data not shown). Thus, we hypothesized that irisin may induce glucose uptake via stimulation of GLUT4 translocation from the perinuclear region to the plasma membrane. A colorimetric assay was used to measure cell surface localization of GLUT4myc. An increase in plasma membrane GLUT4myc was observed in the presence of irisin (Figure 5A). Insulin was used as a positive control for GLUT4 translocation. Irisin-induced GLUT4 translocation was abolished upon treatment with SB202190 (Figure 5B). Irisin-mediated GLUT4 translocation was decreased in p38 MAPK siRNA-transfected cells (Figure 5C). Inhibition of ROS with NAC blocked irisin-mediated GLUT4 translocation, confirmed that ROS is involved in irisin-mediated GLUT4 translocation (Figure 5D). These results imply that irisin stimulates GLUT4 translocation through p38 MAPK activation.

Irisin activates the AMPK and stimulates glucose uptake in primary-cultured myoblasts

To gain insight into the role of irisin in vivo, we examined its effect on primary-cultured myoblast cells. First, we examined its morphological changes during differentiation. After 24 hours, primary-cultured myoblast cells changed to typical fused differentiated status (Figure 6A). To confirm this, we investigated the expression of differentiation marker protein, myogenin. The level of myogenin increased after 24 hours (Figure 6B). The extent of phosphorylation of AMPK, ACC, and p38 MAPK increased in irisin-treated cells compared with control cells (Figure 6C). Compound C abrogated the observed increase of irisin-induced glucose uptake (Figure 6D). Inhibition of p38 MAPK also blocked irisin-induced glucose uptake (Figure 6E). To characterize the components of the AMPK pathway, intracellular Ca^{2+} levels were measured in the presence of irisin. Irisin treatment increased intracellular Ca^{2+} concentration of arrow indicated cells (Figure 6F), pointing to CaMKK as a candidate kinase acting upstream of AMPK, because CaMKK is activated by Ca^{2+}/calmodulin binding. To test this hypothesis, myoblasts

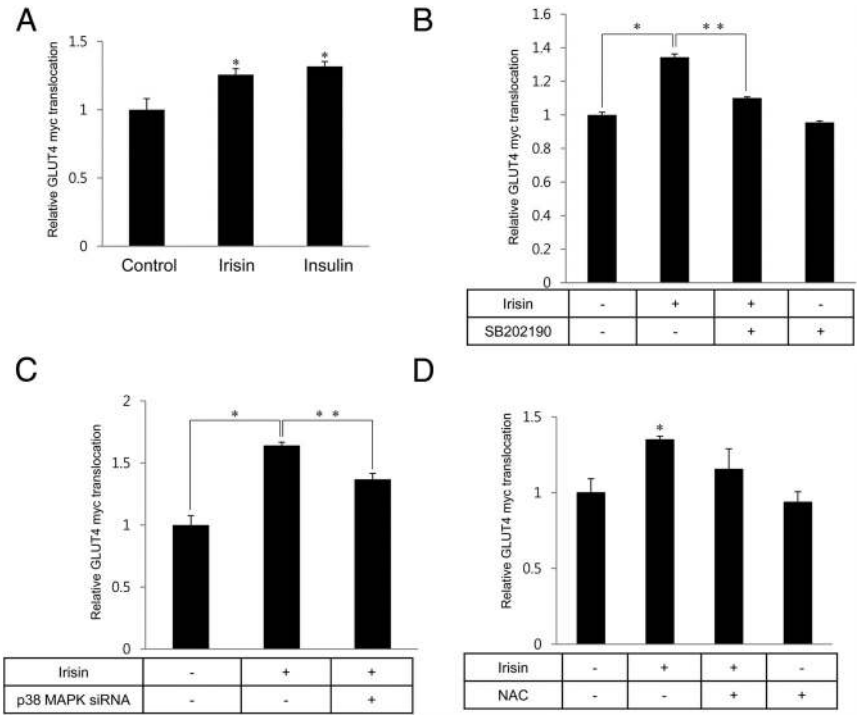

Figure 5. Irisin stimulates GLUT4 translocation. A, Confluent monolayers of myotube cells were incubated with irisin (62 ng/mL) for 60 minutes or insulin for 15 minutes. Cell surface expression of GLUT4myc was detected using an antibody-coupled colorimetric absorbance assay. B, L6 myotube cells were incubated with irisin (62 ng/mL) for 1 hour in the presence of the p38 MAPK inhibitor SB202190 (5 μM), before assaying for GLUT4 translocation. C, L6 myotube cells were transiently transfected with p38 MAPK siRNA (50nM) for 48 hours and then incubated with irisin (62 ng/mL) for 1 hour before assaying for GLUT4 translocation. D, L6 myotube cells were pretreated with NAC for 15 minutes and then incubated with irisin (62 ng/mL) for 1 hour before assaying for GLUT4 translocation. *, $P < .05$ vs basal condition; **, $P < .05$ vs irisin-treated condition.

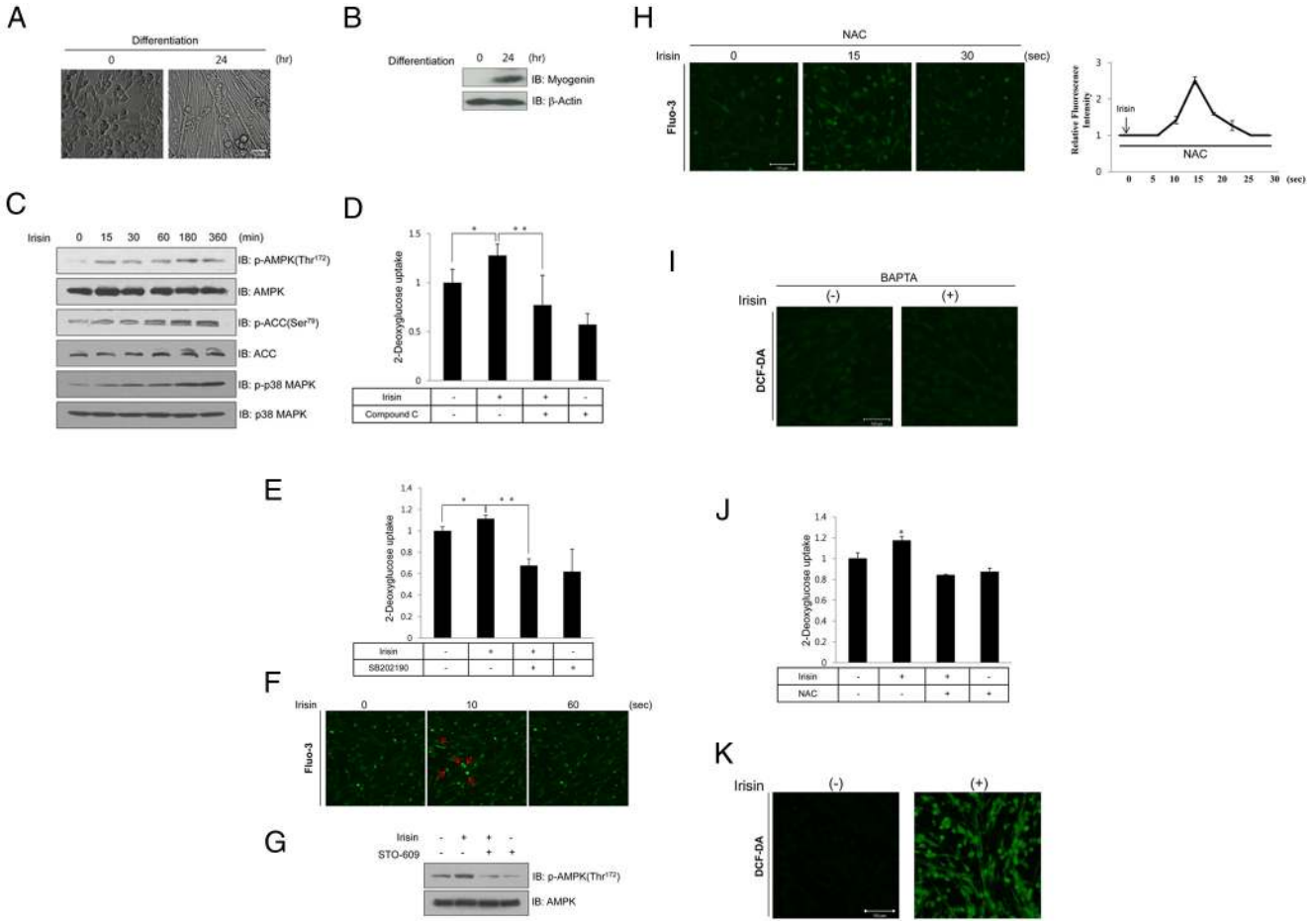

Figure 6. Irisin activates AMPK and stimulates glucose uptake in primary-cultured myoblasts. A, Morphology of differentiated primary-cultured myoblasts. Myoblasts were prepared from quadriceps muscle of 3-day mouse. B, Cell lysates were prepared from myoblasts of 0 and 24 hours of differentiation. The cell lysates were analyzed by Western blotting using antibody against myogenin, whereas β-actin served as controls. C, Differentiated primary-cultured myoblasts cells were stimulated for the indicated times with irisin. Cell lysates were analyzed by Western blotting using antibodies against phospho-AMPK (Thr^{172}), ACC (Ser^{79}), and p38 MAPK, whereas AMPK, ACC, and p38 MAPK served as controls. D, Differentiated primary-cultured myoblast cells were incubated for 1 hour with irisin (62 ng/mL) in the presence of the AMPK inhibitor compound C (2μM), then assayed for glucose uptake. E, Differentiated primary-cultured myoblast cells were incubated for 1 hour with irisin (62 ng/mL) in the presence of the p38 MAPK inhibitor SB202190 (2μM), then assayed for glucose uptake. F, For Ca^{2+} detection, cells were preincubated in Fluo-3 AM (10μM) for 45 minutes. The Ca^{2+} response was measured after treatment of irisin with confocal microscope. Ca^{2+} concentration is correlated with fluorescence intensity. G, Myoblasts were pretreated with the CaMKK inhibitor STO-609 (2μM), then incubated with irisin for 60 minutes. Cell lysates were analyzed by Western blotting using an antibody against phospho-AMPK, whereas AMPK served as a control. H, For Ca^{2+} detection, cells were preincubated in Fluo-3 AM (10μM) for 45 minutes. The Ca^{2+} response was measured after treatment of irisin in the presence of NAC with confocal microscope. I, L6 cells were treated with irisin (62 ng/mL) for 1 hour in the presence of BAPTA. ROS were stained with DCF-DA. Images were captured using a confocal microscope. J, Differentiated primary-cultured myoblast cells were incubated for 1 hour with irisin (62 ng/mL) in the presence of the NAC, then assayed for glucose uptake. K, L6 cells were treated with irisin (62 ng/mL) for 1 hour. ROS were stained with DCF-DA. Images were captured using a confocal microscope. *, $P < .05$ vs basal condition; **, $P < .05$ vs irisin-treated condition.

were pretreated with STO-609, a CaMKK inhibitor, before the addition of irisin. STO-609 blocked irisin-induced AMPK phosphorylation (Figure 6G). Inhibition of ROS with NAC did not change irisin-mediated calcium increase (Figure 6H). On the other hand, blocking the calcium with BAPTA prevented irisin-mediated ROS generation (Figure 6I), indicating that calcium may play as an upstream of ROS in irisin-mediated signaling. Blocking of ROS (Figure 6J) blocked the irisin-mediated glucose uptake in primary cell cultured myoblast. The level of ROS was increased by irisin treatment in the primary myoblast also (Figure 6K). These results demonstrate that the mechanism of glucose uptake induced by irisin involves Ca^{2+}-mediated CaMKK/AMPK pathway in primary cell culture systems.

Discussion

The key finding of this study was that irisin stimulates glucose uptake via AMPKα2-mediated p38 MAPK activation in muscle cells. This was determined directly through observation of glucose uptake in irisin-treated

cells and indirectly through the knockdown of p38 MAPK and by examining GLUT4 translocation in the presence of irisin. Irisin also increased the phosphorylation of AMPKα2 in primary myoblast cells. These results suggest that the hypoglycemic effect of irisin occurs through the regulation of the AMPK pathway in skeletal muscle.

Ever since irisin was identified as a novel myokine, many studies have focused on the characterization of its mechanism of action. Irisin exerts various effects on muscle and nonmuscle tissue via autocrine, paracrine and endocrine pathways. This is interesting because, it means that if administered exogenously, irisin has a promising therapeutic potential. Circulating irisin is present in human plasma, and its concentration is associated with metabolic status (35–38). Moreover, recombinant irisin has been shown to reduce body weight and improve glucose control in mice (26). These in vivo results suggest that irisin may become therapeutically useful for obesity and diabetes. Although there is great interest in the effects of recently identified myokines on metabolic disorders (including this study), the in vitro results here make it difficult to draw definite conclusions about their in vivo functions. The structural stability of irisin in vivo could become a promising candidate for drug development. Future work should address the relationship between irisin and its activity in vivo to fully elucidate the molecular mechanism underlying its function.

In our results, irisin promoted GLUT4 translocation as potent as insulin (Figure 5A). However, irisin did not stimulate glucose uptake as insulin (Figure 1). This discrepancy may be explained by the fact that GLUT4 translocation is necessary factor for glucose uptake, but it is not sufficient factor for glucose uptake. Glucose uptake does not completely due to GLUT4 translocation to the plasma membrane (39). There are some reasons for discrepancy between GLUT4 and glucose uptake. First, there are several kinds of GLUT. Another kinds of GLUT rather than GLUT4 might be also involve in glucose uptake. Second, the degree of glucose uptake is affected by both GLUT4 translocation and GLUT intrinsic activity. Thus, translocation of GLUT4 to the plasma membrane does not entirely account for glucose uptake. In addition, in our experiment, irisin increased glucose uptake at best 30%. Many previous articles demonstrated that activation of AMPK potentiated insulin sensitivity (40, 41). Combined together with our data about AMPK phosphorylation due to irisin, our results suggested that irisin may have physiological importance via its insulin sensitizing effect, even though it increased glucose uptake very little.

One study reported that a lipid-lowering drug, simvastatin, increased irisin concentration in vivo and in vitro (35). Other study, at the same time, reported that there was no correlation between circulation level of irisin at type 2 diabetes (42). Because irisin was reported to be involved in exercise-induced fat browning, research has been focused on the role of PGC1α. Thus, PGC1α-irisin axis is a part of thermogenesis for therapeutics for metabolic diseases, such as diabetes and obesity. Molecule, such as irisin, identified as novel AMPK activator in this study, may have beneficial glucose-regulating effects in low concentration, as well as thermogenesis process.

There is still some controversy surrounding the exact mechanism of irisin activity, specifically with respect to its expression and receptor. One study demonstrated that irisin is expressed in skeletal muscle, the heart, and the cerebellum (43). Together with the finding that FNDC5, the membrane protein that is cleaved to form irisin, is detected in skeletal muscle, indicates that a major site of irisin function may be skeletal muscle. In addition, irisin activity was shown in vivo in very low concentration ranges (21), suggesting the existence of an irisin receptor. The crystal structure of the FNDC5 ectodomain was shown to correspond to irisin (44). This implies that the irisin receptor and soluble irisin may work by binding to a receptor that is yet to be identified. The identity of the irisin receptor has not been explored thus far. Future studies should be focused on characterization of the irisin receptor's existence and function. Together, irisin activates glucose uptake in the skeletal muscles via calcium/ROS-mediated AMPK pathway. P38 MAPK was involved in irisin-mediated glucose uptake in the AMPK downstream pathway. Therefore, we concluded that irisin had beneficial effect in skeletal muscles via AMPK-related pathway.

In summary, irisin was shown to stimulate glucose uptake via AMPKα2 activation in muscle cells in a mechanism likely involving p38 MAPK-GLUT4 translocation. These findings provide insight into the hypoglycemic functions of irisin, and could potentially become the focus of future research on myokines into the treatment of diabetes.

Acknowledgments

Address all correspondence and requests for reprints to: Hyeon Soo Kim, MD, PhD, Korea University College of Medicine, 126-1, Anam-dong 5-ga, Seongbuk-gu, Seoul 136-701, Korea. E-mail: anatomykim@ korea.ac.kr.

This work was supported by the National Research Foundation of Korea Grant NRF-2013R1A2A2A05004796, funded by the Korean government.

Disclosure Summary: The authors have nothing to disclose.

References

1. **Hardie DG, Carling D.** The AMP-activated protein kinase–fuel gauge of the mammalian cell? *Eur J Biochem*. 1997;246:259–273.

2. **Sakamoto K, McCarthy A, Smith D, et al.** Deficiency of LK1 in skeletal muscle prevents AMPK activation and glucose uptake during contraction. *EMBO J*. 2005;24:1810–1820.
3. **Koh HJ, Arnolds DE, Fujii N, et al.** Skeletal muscle-selective knockout of LKB1 increases insulin sensitivity, improves glucose homeostasis, and decreases TRB3. *Mol Cell Biol*. 2006;26:8217–8227.
4. **Woods A, Dickerson K, Heath R, et al.** Ca^{2+}/calmodulin-dependent protein kinase kinase-β acts upstream of AMP-activated protein kinase in mammalian cells. *Cell Metab*. 2005;2:21–33.
5. **Hawley SA, Pan DA, Mustard KJ, et al.** Calmodulin-dependent protein kinase kinase-β is an alternative upstream kinase for AMP-activated protein kinase. *Cell Metab*. 2005;2:9–19.
6. **Hayashi T, Hirshman MF, Kurth EJ, Winder WW, Goodyear LJ.** Evidence for 5′ AMP-activated protein kinase mediation of the effect of muscle contraction on glucose transport. *Diabetes*. 1998;47:1369–1373.
7. **Mu J, Brozinick JT Jr, Valladares O, Bucan M, Birnbaum MJ.** A role for AMP-activated protein kinase in contraction- and hypoxia-regulated glucose transport in skeletal muscle. *Mol Cell*. 2001;7:1085–1094.
8. **Tsao TS, Burcelin R, Katz EB, Huang L, Charron MJ.** Enhanced insulin action due to targeted GLUT4 overexpression exclusively in muscle. *Diabetes*. 1996;45:28–36.
9. **Tsao TS, Li J, Chang KS, et al.** Metabolic adaptations in skeletal muscle overexpressing GLUT4: effects on muscle and physical activity. *FASEB J*. 2001;15:958–969.
10. **Rossetti L, Stenbit AE, Chen W, et al.** Peripheral but not hepatic insulin resistance in mice with one disrupted allele of the glucose transporter type 4 (GLUT4) gene. *J Clinic Invest*. 1997;100:1831–1839.
11. **Shan T, Liang X, Bi P, Kuang S.** Myostatin knockout drives browning of white adipose tissue through activating the AMPK-PGC1α-Fndc5 pathway in muscle. *FASEB J*. 2013;27:1981–1989.
12. **Pedersen BK.** Muscles and their myokines. *J Exp Bio*. 2011;214:337–346.
13. **Pedersen BK, Akerstrom TC, Nielsen AR, Fischer CP.** Role of myokines in exercise and metabolism. *J Appl Physiol*. 2007;103,1093–1098.
14. **Pedersen BK, Febbraio MA.** Muscle as an endocrine organ: focus on muscle-derived interleukin-6. *Physiol Rev*. 2008;88:1379–1406.
15. **Nishimura T, Nakatake Y, Konishi M, Itoh N.** Identification of a novel FGF, FGF-21, preferentially expressed in the liver. *Biochim Biophys Acta*. 2000;1492(1):203–206.
16. **Oshima Y, Ouchi N, Sato K, Izumiya Y, Pimentel DR, Walsh K.** Follistatin-like 1 is an Akt-regulated cardio protective factor that is secreted by the heart. *Circulation*. 2008;117:3099–3108.
17. **Broholm C, Mortensen OH, Nielsen S, et al.** Exercise induces expression of leukaemia inhibitory factor in human skeletal muscle. *J Physiol*. 2008;586:2195–2201.
18. **Haugen F, Norheim F, Lian H, et al.** IL-7 is expressed and secreted by human skeletal muscle cells. *Am J Physiol Cell Physiol*. 2010;298:C807–C816.
19. **Grabstein KH, Eisenman J, Shanebeck K, et al.** Cloning of a T cell growth factor that interacts with the β chain of the interleukin-2 receptor. *Science*. 1994;264:965–968.
20. **Nishizawa H, Matsuda M, Yamada Y, et al.** Musclin, a novel skeletal muscle-derived secretory factor. *J Biol Chem*. 2004;279:19391–19395.
21. **Boström P, Wu J, Jedrychowski MP, et al.** A PGC1-α-dependent myokine that drives brown-fat-like development of white fat and thermogenesis. *Nature*. 2012;481:463–468.
22. **Henriksen T, Green C, Pedersen BK.** Myokines in myogenesis and health. *Recent Pat Biotechnol*. 2012;6:167–171.
23. **Pedersen L, Hojman P.** Muscle-to-organ cross talk mediated by myokines. *Adipocyte*. 2012;1:164–167.
24. **Wang S, Mu J, Fan Z, et al.** Insulin-like growth factor 1 can promote the osteogenic differentiation and osteogenesis of stem cells from apical papilla. *Stem Cell Res*. 2012;8:346–356.
25. **Ouchi N, Oshima Y, Ohashi K, et al.** Follistatin-like 1, a secreted muscle protein, promotes endothelial cell function and revascularization in ischemic tissue through a nitric-oxide synthase-dependent mechanism. *J Biol Chem*. 2008;283:32802–32811.
26. **Zhang Y, Li R, Meng Y, et al.** Irisin stimulates browning of white adipocytes through mitogen-activated protein kinase p38 MAP kinase and ERK MAP kinase signaling. *Diabetes*. 2014;63:514–525.
27. **Hofmann T, Elbelt U, Stengel A.** Irisin as a muscle derived hormone stimulating thermogenesis–a critical update. *Peptides*. 2014;54:89–100.
28. **Moreno-Navarrete JM, Ortega F, Serrano M, et al.** Irisin is expressed and produced by human muscle and adipose tissue in association with obesity and insulin resistance. *J Clin Endocrinol Metab*. 2013;98:E769–E778.
29. **Shafique E, Choy WC, Liu Y, et al.** Oxidative stress improves coronary endothelial function through activation of the pro-survival kinase AMPK. *Aging (Albany NY)*. 2013;5(7):515–530.
30. **Sandström ME, Zhang SJ, Bruton J, et al.** Role of reactive oxygen species in contraction-mediated glucose transport in mouse skeletal muscle. *J Physiol*. 2006;575:251–262.
31. **Lanna A, Henson SM, Escors D, Akbar AN.** The kinase p38 activated by the metabolic regulator AMPK and scaffold TAB1 drives the senescence of human T cells. *Nat Immunol*. 2014;15(10):965–972.
32. **Hsu YC, Meng X, Ou L, Ip MM.** Activation of the AMP-activated protein kinase-p38 MAP kinase pathway mediates apoptosis induced by conjugated linoleic acid in p53-mutant mouse mammary tumor cells. *Cell Signal*. 2010;22(4):590–599.
33. **Niu W, Huang C, Nawaz Z, et al.** Maturation of the regulation of GLUT4 activity by p38 MAPK during L6 cell myogenesis. *J Biol Chem*. 2003;278(20):17953–17962.
34. **Somwar R, Kim DY, Sweeney G, et al.** GLUT4 translocation precedes the stimulation of glucose uptake by insulin in muscle cells: potential activation of GLUT4 via p38 mitogen-activated protein kinase. *Biochem J*. 2001;359(pt 3):639–649.
35. **Gouni-Berthold I, Berthold HK, Huh JY, et al.** Effects of lipid-lowering drugs on irisin in human subjects in vivo and in human skeletal muscle cells ex vivo. *PLoS One*. 2013;8:e72858.
36. **Park KH, Zaichenko L, Brinkoetter M, et al.** Circulating irisin in relation to insulin resistance and the metabolic syndrome. *J Clin Endocrinol Metab*. 2013;98:4899–4907.
37. **Zhang HJ, Zhang XF, Ma ZM, et al.** Irisin is inversely associated with intrahepatic triglyceride contents in obese adults. *J Hepatol*. 2013;59:557–562.
38. **Vamvini MT, Aronis KN, Panagiotou G, et al.** Irisin mRNA And circulating levels in relation to other myokines in healthy and morbidly obese humans. *Eur J Endocrinol*. 2013;169:829–834.
39. **Zierler K.** Does insulin-induced increase in the amount of plasma membrane GLUTs quantitatively account for insulin-induced increase in glucose uptake? *Diabetologia*. 1998;41:724–730.
40. **Carey AL, Steinberg GR, Macaulay SL, et al.** Interleukin-6 increases insulin-stimulated glucose disposal in humans and glucose uptake and fatty acid oxidation in vitro via AMP-activated protein kinase. *Diabetes*. 2006;55(10):2688–2697.
41. **Lee WJ, Song KH, Koh EH, et al.** α-Lipoic acid increases insulin sensitivity by activating AMPK in skeletal muscle. *Biochem Biophys Res Commun*. 2005;8:332(3):885–891.
42. **Yang M, Chen P, Jin H, et al.** Circulating levels of irisin in middle-aged first-degree relatives of type 2 diabetes mellitus — correlation with pancreaticβ-cell function. *Diabetol Metab Syndr*. 2014;6:133.
43. **Dun SL, Lyu RM, Chen YH, Chang JK, Luo JJ, Dun NJ.** Irisin-immunoreactivity in neural and non-neural cells of the rodent. *Neuroscience*. 2013;240:155–162.
44. **Schumacher MA, Chinnam N, Ohashi T, Shah RS, Erickson H.** Structure of irisin reveals a novel intersubunit β-sheet fibronectin (FNIII) dimer: implications for receptor activation. *J Biol Chem*. 2013;288:33738–33744.